J|A|C|S ARTICLES

Published on Web 04/05/2010

Synthesis, Structural Investigations, Hydrogen−Deuterium Exchange Studies, and Molecular Modeling of Conformationally Stablilized Aromatic Oligoamides

Yan Yan,[†] Bo Qin,[†] Changliang Ren,[†] Xiuying Chen,[‡] Yeow Kwan Yip,[†] Ruijuan Ye,[†] Dawei Zhang,[§] Haibin Su,[‡] and Huaqiang Zeng*,[†]

Department of Chemistry and MedChem Programme, National University of Singapore, 3 Science Drive 3, Singapore, 117543, Department of Materials Science, Nanyang Technological University, 50 Nanyang Avenue, Singapore, 639798, and Department of Chemistry and Biological Chemistry, Nanyang Technological University, 21 Nanyang Link, Singapore, 637371

Received February 2, 2010; E-mail: chmzh@nus.edu.sg

Abstract: Biasing the conformational preferences of aromatic oligoamides by internally placing intramolecular hydrogen bonds has led to a series of stably folded molecular strands. This article presents the results from extensive solid-state, solution, and computational studies on these folding oligomers. Depending on its backbone length, an oligoamide adopts a crescent or helical conformation. Surprisingly, despite the highly repetitive nature of the backbone, the internally placed, otherwise very similar intramolecular hydrogen bonds showed significantly different stabilities as demonstrated by hydrogen−deuterium exchange data. It was also observed that the hydrogen-bonding strength can be tuned by adjusting the substituents attached to the exterior of the aromatic backbones. Examining the amide hydrogen−deuterium exchange rates of trimers revealed that a six-membered hydrogen bond nearing the ester end is the weakest among all the four intramolecular hydrogen bonds of a molecule. This observation was verified by *ab initio* quantum mechanical calculations at the level of B3LYP/6-31G*. Such a "weak point" creates the "battle of the bulge" where backbone twisting is centered, which is consistently observed in the solid-state structures of the four trimer molecules studied. In the solid state, the oligomers assemble into interesting one-dimensional structures. A pronounced columnar packing of short oligomers (i.e., dimers, trimers, and tetramer) and channel-like, potentially ion-conducting stacks of longer oligomers (i.e., tetramer, pentamer, and hexamer) were observed.

Introduction

Oligomers that adopt stable, compact conformations have been coined as "foldamers"[1a] that are largely inspired by naturally occurring folding biomolecules including proteins and DNAs. An effective strategy in the designs of foldamers[1,2] involves biasing the preferred conformations of synthetic oligomers by incorporating a multitude of noncovalent interactions such as hydrogen-bonding (H-bonding), solvophobic, $\pi-\pi$ stacking, and metal coordination bonds. Helical structures[3,4] appear to occupy a privileged position among the folding patterns observed in reported foldamers. The progress made so far in designing helical foldamers has allowed a number of functionalities to be incorporated into various structural designs. As such, folding helices endowed with diverse properties have been extensively investigated in recent years that can (1) bind either neutral (saccharides,[4g,h,5−5d] water,[3f,5e−g] and other small molecules[5h,i]) or ionic species,[4i,5j−r] (2) form vesicles and organogels,[6a,b] (3) catalyze reactions[2n,6c] or serve as reactive sieves.[6d−f] (4) act as ion transporters across cell membranes,[6g,h] (5) penetrate cell membranes,[6i] (6) enhance protein stability toward proteolysis[6j] or DNA G-quartet stability,[6k] (7) inhibit protein−protein[2b,7a−h] or protein−membrane[7i−l] interactions, and (8) kill bacteria.[7m−q]

A recently emerged concept in designing sophisticated helical foldamers explores the proper use of multiply centered intramolecular H-bonds of varying types to constrain the backbones of aromatic oligoamides and their analogues such as aromatic oligohydrazides and oligoureas. Manipulating the folding of these aromatic oligomers on the basis of this strategy has allowed the creation of foldamers with a helically wrapped interior cavity of as small as 1.4 Å[8] and as large as 30 Å in radius[3d] (Chart 1). This concept can be traced back to the pioneering work on pyridine amide oligomers by Hamilton,[3a,b,9a]

[†] National University of Singapore.
[‡] Department of Materials Science, Nanyang Technological University.
[§] Department of Chemistry and Biological Chemistry, Nanyang Technological University.

(1) (a) Gellman, S. H. *Acc. Chem. Res.* **1998**, *31*, 173. (b) Stigers, K. D.; Soth, M. J.; Nowick, J. S. *Curr. Opin. Chem. Biol.* **1999**, *3*, 714. (c) Gong, B. *Chem.—Eur. J.* **2001**, *7*, 4336. (d) Hill, D. J.; Mio, M. J.; Prince, R. B.; Hughes, T. S.; Moore, J. S. *Chem. Rev.* **2001**, *101*, 3893. (e) Cheng, R. P.; Gellman, S. H.; DeGrado, W. F. *Chem. Rev.* **2001**, *101*, 3219. (f) Cubberley, M. S.; Iverson, B. L. *Curr. Opin. Chem. Biol.* **2001**, *5*, 650. (g) Archer, E. A.; Gong, H. G.; Krische, M. J. *Tetrahedron* **2001**, *57*, 1139. (h) Sanford, A. R.; Gong, B. *Curr. Org. Chem.* **2003**, *7*, 1649. (i) Sanford, A. R.; Yamato, K.; Yang, X.; Yuan, L.; Han, Y.; Gong, B. *Eur. J. Biochem.* **2004**, *271*, 1416. (j) Schmuck, C. *Angew. Chem., Int. Ed.* **2003**, *42*, 2448. (k) Huc, I. *Eur. J. Org. Chem.* **2004**, 17. (l) Cheng, R. P. *Curr. Opin. Struct. Biol.* **2004**, *14*, 512. (m) Licini, G.; Prins, L. J.; Scrimin, P. *Eur. J. Org. Chem.* **2005**, 969. (n) Li, Z. T.; Hou, J. L.; Li, C.; Yi, H. P. *Chem. Asian J.* **2006**, *1*, 766. (o) Sanji, T.; Tanaka, M. *J. Synth. Org. Chem. Jpn.* **2006**, *64*, 947.

Chart 1

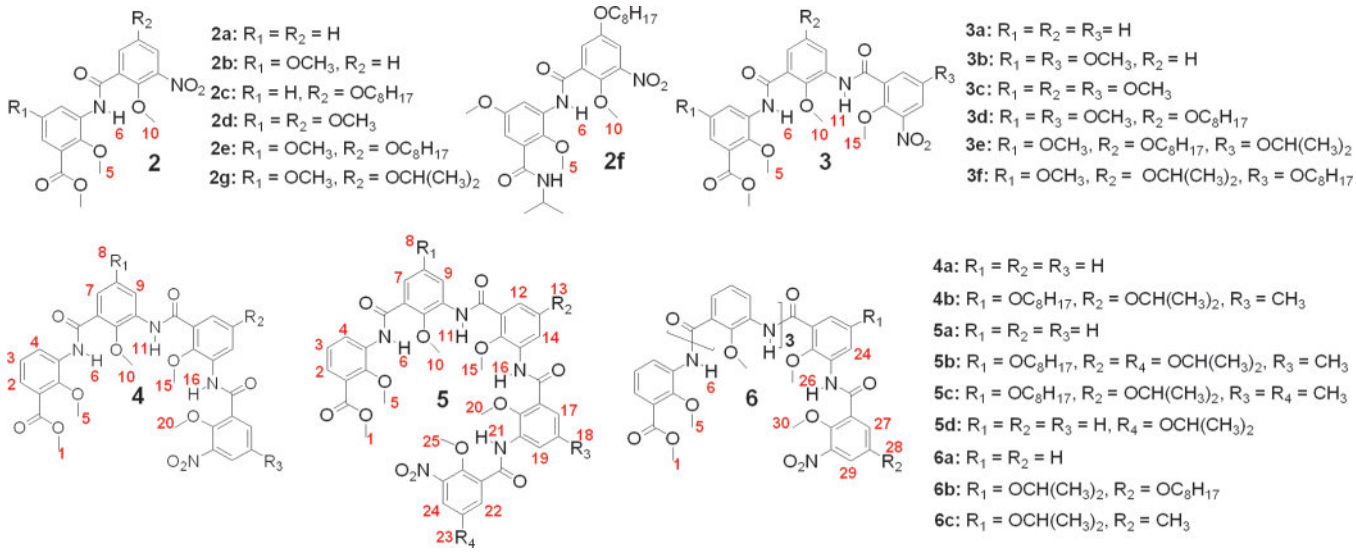

aromatic oligoamides/ureas/hydrazides/arylene ethynylenes by Gong,[3d,10] aromatic oligoureas by Zimmerman,[9b] pyridine amide oligomers and quinoline carboxamide oligomers by Lehn,[3c,11a−d] and Huc,[3c,e,f,m,5e−g,6i,k,11a,b,e−r] followed by the active explorations on aromatic amides/hydrazides by Li,[4g,5b,d,m,n,6a,b,12a−c] Chen,[6f,12d−g] and others.[3g,12h−j]

By including novel building blocks and H-bonding patterns, we[8,13] and others[5n,10k,12a,b,i] have been interested in further developing the corresponding field. Specifically, the structural and physical properties of a new family of backbone-rigidified oligoamide strands represented by hexamer **6** have been investigated. The folding of these oligomers is enforced by an inward-pointing, continuous H-bonding network and is characterized by a helical periodicity of five repeating units per turn that encloses a helical cavity of 1.4 Å in radius.[8] While these methoxy-containing oligomers with sufficiently long backbones (i.e., **5a** and **6a**) have been shown by us to adopt a stable helical conformation,[8] the corresponding demethylated phenolic oligoamides, consisting of up to four monomeric residues and with interiors decorated by hydroxyl groups, display a linear-to-turn conformational switching induced by deprotonation of phenolic hydroxyl groups.[12i] In view of the fact that the radius of the majority of cations stays below 1.4 Å, the selective demethylation of one or more methoxy groups in an oligomer such as **6** and subsequent deprotonation of the resulting phenolic hydroxyl groups should open up the cavity for helically wrapping cations of varying types (i.e., Na^+ and K^+).[2l,m,14]

In this article, we focus on shedding additional insights into the largely unexplored structural features (backbone bending, columnar packing, and potential channel formation) and on

(2) (a) Li, X.; Yang, D. *Chem. Commun.* **2006**, 3367. (b) Goodman, C. M.; Choi, S.; Shandler, S.; DeGrado, W. F. *Nat. Chem. Biol.* **2007**, *3*, 252. (c) Hecht, S. M.; Huc, I. *Foldamers: Structure, Properties and Applications*; Wiley-VCH: Weinheim, Germany, 2007. (d) Gong, B.; Sanford, A. R.; Ferguson, J. S. *In Oligomers Polymer Composties Molecular Imprinting*; Springer-Verlag Berlin: Berlin, 2007; Vol. 206. (e) Li, C. Z.; Jiang, X. K.; Li, Z. T.; Gao, X.; Wang, Q. R. *Chin. J. Org. Chem.* **2007**, *27*, 188. (f) Haldar, D. *Curr. Org. Synth.* **2008**, *5*, 61. (g) Li, Z. T.; Hou, J. L.; Li, C. *Acc. Chem. Res.* **2008**, *41*, 1343. (h) Horne, W. S.; Gellman, S. H. *Acc. Chem. Res.* **2008**, *41*, 1399. (i) Gong, B. *Acc. Chem. Res.* **2008**, *41*, 1376. (j) Li, X.; Wu, Y.-D.; Yang, D. *Acc. Chem. Res.* **2008**, *41*, 1428. (k) Haldar, D.; Schmuck, C. *Chem. Soc. Rev.* **2009**, *38*, 363. (l) Piguet, C.; Bernardinelli, G.; Hopfgartner, G. *Chem. Rev.* **1997**, *97*, 2005. (m) Albrecht, M. *Chem. Rev.* **2001**, *101*, 3457. (n) Hooley, R. J.; Rebek, J., Jr. *Chem. Biol.* **2009**, *16*, 255. (o) Baptiste, B.; Godde, F.; Huc, I. *ChemBioChem* **2009**, *10*, 1765.

(3) For some selected folding helices supported by solid-state structures, see: (a) Hamuro, Y.; Geib, S. J.; Hamilton, A. D. *Angew. Chem., Int. Ed.* **1994**, *33*, 446. (b) Hamuro, Y.; Geib, S. J.; Hamilton, A. D. *J. Am. Chem. Soc.* **1997**, *119*, 10587. (c) Berl, V.; Huc, I.; Khoury, R. G.; Krische, M. J.; Lehn, J. M. *Nature* **2000**, *407*, 720. (d) Gong, B.; Zeng, H. Q.; Zhu, J.; Yuan, L. H.; Han, Y. H.; Cheng, S. Z.; Furukawa, M.; Parra, R. D.; Kovalevsky, A. Y.; Mills, J. L.; Skrzypczak-Jankun, E.; Martinovic, S.; Smith, R. D.; Zheng, C.; Szyperski, T.; Zeng, X. C. *Proc. Natl. Acad. Sci. U.S.A.* **2002**, *99*, 11583. (e) Jiang, H.; Léger, J.-M.; Huc, I. *J. Am. Chem. Soc.* **2003**, *125*, 3448. (f) Garric, J.; Léger, J.-M.; Huc, I. *Angew. Chem., Int. Ed.* **2005**, *44*, 1954. (g) Tie, C.; Gallucci, J. C.; Parquette, J. R. *J. Am. Chem. Soc.* **2006**, *128*, 1162. (h) Wu, C. W.; Kirshenbaum, K.; Sanborn, T. J.; Patch, J. A.; Huang, K.; Dill, K. A.; Zuckermann, R. N.; Barron, A. E. *J. Am. Chem. Soc.* **2003**, *125*, 13525. (i) Yang, D.; Zhang, Y.-H.; Li, B.; Zhang, D.-W.; Chan, J. C.-Y.; Zhu, N.-Y.; Luo, S.-W.; Wu, Y.-D. *J. Am. Chem. Soc.* **2004**, *126*, 6956. (j) Choi, S. H.; Guzei, I. A.; Gellman, S. H. *J. Am. Chem. Soc.* **2007**, *129*, 13780. (k) Schmitt, M. A.; Choi, S. H.; Guzei, I. A.; Gellman, S. H. *J. Am. Chem. Soc.* **2006**, *128*, 4538. (l) Horne, W. S.; Price, J. L.; Keck, J. L.; Gellman, S. H. *J. Am. Chem. Soc.* **2007**, *129*, 4178. (m) Gan, Q.; Bao, C. Y.; Kauffmann, B.; Grelard, A.; Xiang, J. F.; Liu, S. H.; Huc, I.; Jiang, H. *Angew. Chem., Int. Ed.* **2008**, *47*, 1715. (n) Prabhakaran, P.; Kale, S. S.; Puranik, V. G.; Rajamohanan, P. R.; Chetina, O.; Howard, J. A. K.; Hofmann, H. J.; Sanjayan, G. J. *J. Am. Chem. Soc.* **2008**, *130*, 17743. (o) Hayen, A.; Schmitt, M. A.; Ngassa, F. N.; Thomasson, K. A.; Gellman, S. H. *Angew. Chem., Int. Ed.* **2004**, *43*, 505.

(4) For some selected folding helices with solid-state structures remaining unknown, see: (a) Cuccia, L. A.; Lehn, J.-M.; Homo, J.-C.; Schmutz, M. *Angew. Chem., Int. Ed.* **2000**, *39*, 233. (b) Yang, X. W.; Brown, A. L.; Furukawa, M.; Li, S.; Gardinier, W. E.; Bukowski, E. J.; Bright, F. V.; Zheng, C.; Zeng, X. C.; Gong, B. *Chem. Commun.* **2003**, 56. (c) De Pol, S.; Zorn, C.; Klein, C. D.; Zerbe, O.; Reiser, O. *Angew. Chem., Int. Ed.* **2004**, *43*, 511. (d) Dolain, C.; Maurizot, V.; Huc, I. *Angew. Chem., Int. Ed.* **2003**, *42*, 2738. (e) Gorp, J. J. v.; Vekemans, J. A. J. M.; Meijer, E. W. *Chem. Commun.* **2004**, 60. (f) Yang, X. W.; Yuan, L. H.; Yamamoto, K.; Brown, A. L.; Feng, W.; Furukawa, M.; Zeng, X. C.; Gong, B. *J. Am. Chem. Soc.* **2004**, *126*, 3148. (g) Hou, J. L.; Shao, X. B.; Chen, G. J.; Zhou, Y. X.; Jiang, X. K.; Li, Z. T. *J. Am. Chem. Soc.* **2004**, *126*, 12386. (h) Abe, H.; Masuda, N.; Waki, M.; Inouye, M. *J. Am. Chem. Soc.* **2005**, *127*, 16189. (i) Zhao, Y.; Zhong, Z. *J. Am. Chem. Soc.* **2005**, *127*, 17894. (j) Sinkeldam, R. W.; Hoeben, F. J. M.; Pouderoijen, M. J.; DeCat, I.; Zhang, J.; Furukawa, S.; DeFeyter, S.; Vekemans, J. A. J. M.; Meijer, E. W. *J. Am. Chem. Soc.* **2006**, *128*, 16113. (k) Khan, A.; Kaiser, C.; Hecht, S. *Angew. Chem., Int. Ed.* **2006**, *45*, 1878. (l) Zhao, Y.; Zhong, Z. Q.; Ryu, E. H. *J. Am. Chem. Soc.* **2007**, *129*, 218.

revealing the location-dependent strength of multiply centered intramolecular H-bonds, which play a critical role in the folding of these oligomers. First, ^{1}H NMR and X-ray diffraction were used to establish the folding of these conformationally rigid aromatic oligomers. Second, amide hydrogen−deuterium (H−D) exchange studies were used to infer the strengths of various intramolecular H-bonds placed at different locations along a backbone, results from which have allowed us to pinpoint the local conformational weakness along the oligoamide backbone. The conclusion from H−D exchange was confirmed by the crystal structures of a series of oligomers, which allow a qualitative correlation between the conformational stability of the H-bond-enforced backbones and the strength of individual H-bonds that are sensitive to local structural environments.[10e,13] The correlation derived from H−D studies and solid-state investigations was substantiated by results from *ab initio* calculations at the level of B3LYP/6-31G*. Examining the assembly of the oligomers in the solid state revealed a columnar

(5) Inouye, M.; Waki, M.; Abe, H. *J. Am. Chem. Soc.* **2004**, *126*, 2022. (b) Li, C.; Wang, G. T.; Yi, H. P.; Jiang, X. K.; Li, Z. T.; Wang, R. X. *Org. Lett.* **2007**, *9*, 1797. (c) Waki, M.; Abe, H.; Inouye, M. *Angew. Chem., Int. Ed.* **2007**, *46*, 3059. (d) Yi, H.-P.; Shao, X.-B.; Hou, J.-L.; Li, C.; Jiang, X.-K.; Li, Z.-T. *New J. Chem.* **2005**, *29*, 1213. (e) Berl, V.; Huc, I.; Khoury, R. G.; Lehn, J.-M. *Chem.—Eur. J.* **2001**, *7*, 2810. (f) Huc, I.; Maurizot, V.; Gornitzka, H.; Léger, J.-M. *Chem. Commun.* **2002**, 578. (g) Garric, J.; Léger, J.-M.; Huc, I. *Chem.—Eur. J.* **2007**, *13*, 8454. (h) Prince, R. B.; Barnes, S. A.; Moore, J. S. *J. Am. Chem. Soc.* **2000**, *122*, 2758. (i) Nishinaga, T.; Tanatani, A.; Oh, K.; Moore, J. S. *J. Am. Chem. Soc.* **2002**, *124*, 5934. (j) Chang, K. J.; Kang, B. N.; Lee, M. H.; Jeong, K. S. *J. Am. Chem. Soc.* **2005**, *127*, 12214. (k) Bell, T.; Jousselin, H. *Nature* **1994**, *367*, 441. (l) Hou, J. L.; Jia, M. X.; Jiang, X. K.; Li, Z. T.; Chen, G. J. *J. Org. Chem.* **2004**, *69*, 6228. (m) Li, C.; Ren, S.-F.; Hou, J.-L.; Yi, H.-P.; Zhu, S.-Z.; Jiang, X.-K.; Li, Z.-T. *Angew. Chem., Int. Ed.* **2005**, *44*, 5725. (n) Yi, H. P.; Li, C.; Hou, J. L.; Jiang, X. K.; Li, Z. T. *Tetrahedron* **2005**, *61*, 7974. (o) Zhao, Y.; Zhong, Z. Q. *J. Am. Chem. Soc.* **2006**, *128*, 9988. (p) Kim, U. I.; Suk, J. M.; Naidu, V. R.; Jeong, K. S. *Chem.—Eur. J.* **2008**, *14*, 11406. (q) Naidu, V. R.; Kim, M. C.; Suk, J. M.; Kim, H. J.; Lee, M.; Sim, E.; Jeong, K. S. *Org. Lett.* **2008**, *10*, 5373. (r) Zhong, Z. Q.; Zhao, Y. *Org. Lett.* **2007**, *9*, 2891.

(6) (a) Cai, W.; Wang, G. T.; Xu, Y. X.; Jiang, X. K.; Li, Z. T. *J. Am. Chem. Soc.* **2008**, *130*, 6936. (b) Cai, W.; Wang, G. T.; Du, P.; Wang, R. X.; Jiang, X. K.; Li, Z. T. *J. Am. Chem. Soc.* **2008**, *130*, 13450. (c) Muller, M. M.; Windsor, M. A.; Pomerantz, W. C.; Gellman, S. H.; Hilvert, D. *Angew. Chem., Int. Ed.* **2009**, *48*, 922. (d) Smaldone, R. A.; Moore, J. S. *J. Am. Chem. Soc.* **2007**, *129*, 5444. (e) Srinivas, K.; Kauffmann, B.; Dolain, C.; Léger, J. M.; Ghosez, L.; Huc, I. *J. Am. Chem. Soc.* **2008**, *130*, 13210. (f) Hu, H. Y.; Xiang, J. F.; Cao, J.; Chen, C. F. *Org. Lett.* **2008**, *10*, 5035. (g) Burkhart, B. M.; Li, N.; Langs, D. A.; Pangborn, W. A.; Duax, W. L. *Proc. Natl. Acad. Sci. U.S.A.* **1998**, *95*, 12950. (h) Burkhart, B. M.; Gassman, R. M.; Langs, D. A.; Pangborn, W. A.; Duax, W. L.; Pletnev, V. *Biopolymers* **1999**, *51*, 129. (i) Gillies, E. R.; Deiss, F.; Staedel, C.; Schmitter, J. M.; Huc, I. *Angew. Chem., Int. Ed.* **2007**, *46*, 4081. (j) Horne, W. S.; Boersma, M. D.; Windsor, M. A.; Gellman, S. H. *Angew. Chem., Int. Ed.* **2008**, *47*, 2853. (k) Shirude, P. S.; Gillies, E. R.; Ladame, S.; Godde, F.; Shin-Ya, K.; Huc, I.; Balasubramanian, S. *J. Am. Chem. Soc.* **2007**, *129*, 11890.

(7) (a) Ferrer, M.; Kapoor, T. M.; Strassmaier, T.; Weissenhorn, W.; Skehel, J. J.; Oprian, D.; Schreiber, S. L.; Wiley, D. C.; Harrison, S. C. *Nat. Struct. Biol.* **1999**, *6*, 953. (b) Patch, J. A.; Barron, A. E. *J. Am. Chem. Soc.* **2003**, *125*, 12092. (c) Yin, H.; Hamilton, A. D. *Angew. Chem., Int. Ed.* **2005**, *44*, 4130. (d) Kritzer, J. A.; Stephens, O. M.; Guarracino, D. A.; Reznik, S. K.; Schepartz, A. *Bioorg. Med. Chem.* **2005**, *13*, 11. (e) Stephens, O. M.; Kim, S.; Welch, B. D.; Hodsdon, M. E.; Kay, M. S.; Schepartz, A. *J. Am. Chem. Soc.* **2005**, *127*, 13126. (f) Kritzer, J. A.; Luedtke, N. W.; Harker, E. A.; Schepartz, A. *J. Am. Chem. Soc.* **2005**, *127*, 14584. (g) Murray, J. K.; Farooqi, B.; Sadowsky, J. D.; Scalf, M.; Freund, W. A.; Smith, L. M.; Chen, J. D.; Gellman, S. H. *J. Am. Chem. Soc.* **2005**, *127*, 13271. (h) Sadowsky, J. D.; Fairlie, W. D.; Hadley, E. B.; Lee, H. S.; Umezawa, N.; Nikolovska-Coleska, Z.; Wang, S. M.; Huang, D. C. S.; Tomita, Y.; Gellman, S. H. *J. Am. Chem. Soc.* **2007**, *129*, 139. (i) Schmitt, M. A.; Weisblum, B.; Gellman, S. H. *J. Am. Chem. Soc.* **2004**, *126*, 6848. (j) Liu, D.; Choi, S.; Chen, B.; Doerksen, R. J.; Clements, D. J.; Winkler, J. D.; Klein, M. L.; DeGrado, W. F. *Angew. Chem., Int. Ed.* **2004**, *43*, 1158. (k) Ishitsuka, Y.; Arnt, L.; Majewski, J.; Frey, S.; Ratajczek, M.; Kjaer, K.; Tew, G. N.; Lee, K. Y. C. *J. Am. Chem. Soc.* **2006**, *128*, 13123. (l) Arnt, L.; Rennie, J. R.; Linser, S.; Willumeit, R.; Tew, G. N. *J. Phys. Chem. B* **2006**, 3527. (m) Hamuro, Y.; Schneider, J. P.; DeGrado, W. F. *J. Am. Chem. Soc.* **1999**, *121*, 12200. (n) Porter, E. A.; Wang, X.; Lee, H. S.; Weisblum, B.; Gellman, S. H. *Nature* **2000**, *404*, 565. (o) Porter, E. A.; Weisblum, B.; Gellman, S. H. *J. Am. Chem. Soc.* **2002**, *124*, 7324. (p) Arvidsson, P. I.; Ryder, N. S.; Weiss, H. M.; Gross, G.; Kretz, O.; Woessner, R.; Seebach, D. *ChemBioChem* **2003**, *4*, 1345. (q) Liu, D.; DeGrado, W. F. *J. Am. Chem. Soc.* **2001**, *123*, 7553.

(8) Yan, Y.; Qin, B.; Shu, Y. Y.; Chen, X. Y.; Yip, Y. K.; Zhang, D. W.; Su, H. B.; Zeng, H. Q. *Org. Lett.* **2009**, *11*, 1201.

(9) (a) Hamuro, Y.; Geib, S. J.; Hamilton, A. D. *J. Am. Chem. Soc.* **1996**, *118*, 7529. (b) Corbin, P. S.; Zimmerman, S. C.; Thiessen, P. A.; Hawryluk, N. A.; Murray, T. J. *J. Am. Chem. Soc.* **2001**, *123*, 10475.

(10) (a) Zhu, J.; Parra, R. D.; Zeng, H. Q.; Skrzypczak-Jankun, E.; Zeng, X. C.; Gong, B. *J. Am. Chem. Soc.* **2000**, *122*, 4219. (b) Parra, R. D.; Zeng, H. Q.; Zhu, J.; Zheng, C.; Zeng, X. C.; Gong, B. *Chem.—Eur. J.* **2001**, *7*, 4352. (c) Parra, R. D.; Furukawa, M.; Gong, B.; Zeng, X. C. *J. Chem. Phys.* **2001**, *115*, 6030. (d) Parra, R. D.; Gong, B.; Zeng, X. C. *J. Chem. Phys.* **2001**, *115*, 6036. (e) Yuan, L. H.; Zeng, H. Q.; Yamato, K.; Sanford, A. R.; Feng, W.; Atreya, H. S.; Sukumaran, D. K.; Szyperski, T.; Gong, B. *J. Am. Chem. Soc.* **2004**, *126*, 16528. (f) Yuan, L.; Feng, W.; Yamato, K.; Sanford, A. R.; Xu, D.; Guo, H.; Gong, B. *J. Am. Chem. Soc.* **2004**, *126*, 11120. (g) Yuan, L. H.; Sanford, A. R.; Feng, W.; Zhang, A. M.; Zhu, J.; Zeng, H. Q.; Yamato, K.; Li, M. F.; Ferguson, J. S.; Gong, B. *J. Org. Chem.* **2005**, *70*, 10660. (h) Sanford, A. R.; Yuan, L.; Feng, W.; Flowersb, K. Y. R. A.; Gong, B. *Chem. Commun.* **2005**, 4720. (i) Zhang, A. M.; Ferguson, J. S.; Yamato, K.; Zheng, C.; Gong, B. *Org. Lett.* **2006**, *8*, 5117. (j) Zhang, A. M.; Han, Y. H.; Yamato, K.; Zeng, X. C.; Gong, B. *Org. Lett.* **2006**, *8*, 803. (k) Zhu, Y. Y.; Li, C.; Li, G. Y.; Jiang, X. K.; Li, Z. T. *J. Org. Chem.* **2008**, *73*, 1745. (l) Zhang, Y. F.; Yamato, K.; Zhong, K.; Zhu, J.; Deng, J. G.; Gong, B. *Org. Lett.* **2008**, *10*, 4339. (m) Helsel, A. J.; Brown, A. L.; Yamato, K.; Feng, W.; Yuan, L. H.; Clements, A. J.; Harding, S. V.; Szabo, G.; Shao, Z. F.; Gong, B. *J. Am. Chem. Soc.* **2008**, *130*, 15784. (n) Yang, L. Q.; Zhong, L. J.; Yamato, K.; Zhang, X. H.; Feng, W.; Deng, P. C.; Yuan, L. H.; Zeng, X. C.; Gong, B. *New J. Chem.* **2009**, *33*, 729.

(11) (a) Berl, V.; Huc, I.; Khoury, R.; Lehn, J.-M. *Chem.—Eur. J.* **2001**, *7*, 2798. (b) Berl, V.; Huc, I.; Khoury, R.; Lehn, J.-M. *Chem.—Eur. J.* **2001**, *7*, 2810. (c) Kolomiets, E.; Berl, V.; Odriozola, I.; Stadler, A. M.; Kyritsakas, N.; Lehn, J. M. *Chem. Commun.* **2003**, 2868. (d) Kolomiets, E.; Berl, V.; Lehn, J. M. *Eur. J. Org. Chem.* **2007**, *13*, 5466. (e) Dolain, C.; Zhan, C. L.; Léger, J. M.; Daniels, L.; Huc, I. *J. Am. Chem. Soc.* **2005**, *127*, 2400. (f) Jiang, H.; Léger, J.-M.; Dolain, C.; Guionneau, P.; Huc, I. *Tetrahedron* **2003**, *59*, 8365. (g) Jiang, H.; Léger, J.-M.; Guionneau, P.; Huc, I. *Org. Lett.* **2004**, *6*, 2985. (h) Jiang, H.; Maurizot, V.; Huc, I. *Tetrahedron* **2004**, *60*, 10029. (i) Jiang, H.; Dolain, C.; Léger, J. M.; Gornitzka, H.; Huc, I. *J. Am. Chem. Soc.* **2004**, *126*, 1034. (j) Maurizot, V.; Dolain, C.; Leydet, Y.; Léger, J.-M.; Guionneau, P.; Huc, I. *J. Am. Chem. Soc.* **2004**, *126*, 10049. (k) Dolain, C.; Grélard, A.; Laguerre, M.; Jiang, H.; Maurizot, V.; Huc, I. *Chem.—Eur. J.* **2005**, *11*, 6135. (l) Dolain, C.; Jiang, H.; Léger, J. M.; Guionneau, P.; Huc, I. *J. Am. Chem. Soc.* **2005**, *127*, 12943. (m) Zhan, C. L.; Léger, J. M.; Huc, I. *Angew. Chem., Int. Ed.* **2006**, *45*, 4625. (n) Haldar, D.; Jiang, H.; Léger, J. M.; Huc, I. *Angew. Chem., Int. Ed.* **2006**, *45*, 5483. (o) Gillies, E. R.; Dolain, C.; Léger, J.-M.; Huc, I. *J. Org. Chem.* **2006**, *71*, 7931. (p) Berni, E.; Dolain, C.; Kauffmann, B.; Léger, J. M.; Zhan, C. L.; Huc, I. *J. Org. Chem.* **2008**, *73*, 2687. (q) Berni, E.; Garric, J.; Lamit, C.; Kauffmann, B.; Léger, J. M.; Huc, I. *Chem. Commun.* **2008**, 1968. (r) Bao, C.; Kauffmann, B.; Gan, Q.; Srinivas, K.; Jiang, H.; Huc, I. *Angew. Chem., Int. Ed.* **2008**, *47*, 4153.

(12) (a) Yi, H.-P.; Wu, J.; Ding, K.-L.; Jiang, X.-K.; Li, Z.-T. *J. Org. Chem.* **2007**, *72*, 870. (b) Hou, J.-L.; Y, H.-P.; Sha, X.-B.; L, C.; W, Z.-Q.; Jian, X.-K.; Wu, L.-Z.; Tung, C.-H.; Li, Z.-T. *Angew. Chem., Int. Ed.* **2006**, *45*, 796. (c) Li, C.; Zhu, Y. Y.; Yi, H. P.; Li, C. Z.; Jiang, Y. K.; Li, Z. T.; Yu, Y. H. *Chem.—Eur. J.* **2007**, *13*, 9990. (d) Hu, Z. Q.; Chen, C. F. *Tetrahedron* **2006**, *62*, 3446. (e) Hu, Z. Q.; Hu, H. Y.; Chen, C. F. *J. Org. Chem.* **2006**, *71*, 1131. (f) Hu, H. Y.; Xiang, J. F.; Yang, Y.; Chen, C. F. *Org. Lett.* **2008**, *10*, 69. (g) Hu, H. Y.; Xiang, J. F.; Yang, Y.; Chen, C. F. *Org. Lett.* **2008**, *10*, 1275. (h) Yu, Q.; Baroni, T. E.; Liable-Sands, L.; Rheingold, A. L.; Borovik, A. S. *Tetrahedron Lett.* **1998**, *39*, 6831. (i) Kanamori, D.; Okamura, T. A.; Yamamoto, H.; Ueyama, N. *Angew. Chem., Int. Ed.* **2005**, *44*, 969. (j) Li, X.; Zhan, C. L.; Wang, Y. B.; Yao, J. N. *Chem. Commun.* **2008**, 2444.

Scheme 1. Synthesis of Monomeric Building Blocks[a]

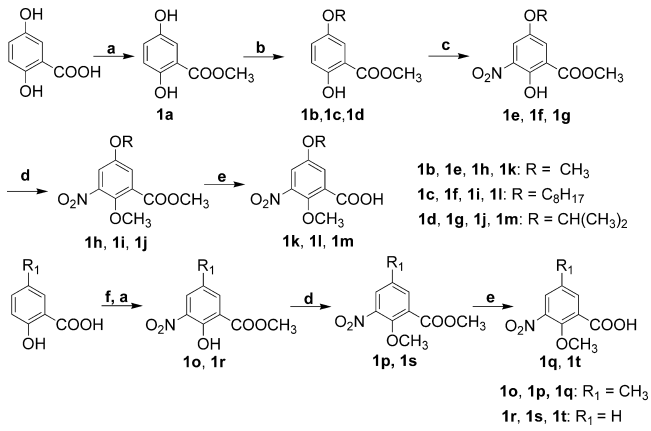

[a] a) conc. H_2SO_4, MeOH, reflux; b) K_2CO_3/RBr (or RI), anhydrous acetone, reflux; c) $Bi(NO_3)_3$, MMT K10, THF; d) K_2CO_3/CH_3I, DMF; e) NaOH, MeOH/H_2O, reflux; f) conc. HNO_3, Conc. H_2SO_4.

packing shared by all of the oligomers ranging from dimer to hexamer. The interplay of $\pi-\pi$ stacking and van der Waals' interactions provide the driving forces for the observed formation of columns. With their persistent shapes, tunable sizes, and tendency to aggregate into column- and channel-like structures, these folding oligomers may serve as novel building blocks for constructing higher-order supramolecular structures with non-collapsible pores and channels capable of conducting ions and small molecules.[10m]

Results and Discussion

Synthesis of Oligoamides 1−6. We recently reported our studies on pentamers **5a** and **5b** and hexamers **6a** and **6b**,[8] demonstrating that these higher oligoamides containing long enough backbones can efficiently fold into a helical conformation to enclose an interior radius of about 1.4 Å. All these four oligoamides and other similar ones described in Schemes 2−4 were synthesized from commercially available salicylic acid, 2,5-dihydroxybenzoic acid and 2-hydroxy-5-methylbenzoic acid in up to 18 steps.

Monomeric building blocks **1k**, **1l**, **1 m**, **1q**, and **1t** were prepared according to Scheme 1. These five building blocks differ from each other only by the remote alkoxyl substituents meta to nitro group. Introduction of these side chains prove critically important in conformational characterization in solution by two-dimensional (2D) NOESY study and in the solid state by X-ray diffraction method.

Among the above five building blocks, **1k**, **1l** and **1m** were prepared after five steps starting from 2,5-dihydroxybenzoic acid. As shown in Scheme 1, esterification in methanol provided methyl ester **1a** in a high yield of ∼90%. The second step involving chemoselective alkylation turned out to be quite sensitive to the solvents used. While the use of DMF produced dialkylated product in both hydroxyl groups, a desirable shifting to the monoalkylation occurred almost exclusively at the hydroxyl group meta to ester group with the use of alkyl iodides/bromides under refluxing conditions in the presence of K_2CO_3 in acetone. Since **1a** has two hydroxyl groups on the same benzene ring, no more than 1.1 equiv of the alkyl iodine (or bromide) was used. This led to a long reaction time and moderate chemical yields (∼60%) for **1b−1d**. Nevertheless, simple flash column chromatography allows the easy purification of the products and recycling of the starting material. This chemoselective alkylation was unambiguously confirmed by the determined crystal structure of **1c** (Figure 5).

Attempted nitrations of **1b−1d** by varying the ratio of conc. nitric acid and conc. sulfuric acid in dichloromethane (CH_2Cl_2) at varying temperatures from −40 to 45 °C invariably led to a mixture of at least three products detectable by TLC, from which the desired products **1e−1g** were obtained in a unacceptable low yield of less than 30%. After testing a few more other conditions (i.e., conc. nitric acid in acetic acid, or slow addition of conc. sulfuric acid into conc. nitric acid containing compounds to be nitrated), the nitration method using montmorillonite impregnated with bismuth nitrate was finally singled out. The condition was very mild, simply involving mixing the compounds to be nitrated (**1b−1d**) with Montmorillonite KSF impregnated with bismuth nitrate in THF at room temperature and stirring the solution for 12 h. Under this condition, a clean reaction producing only **1e−1g** was obtained. It was later found out that a considerable amount of nitrated products was absorbed into solid support Montmorillonite KSF, which can not be efficiently extracted out using CH_2Cl_2. This issue was solved by adding a small amount of acid (1 M HCl) to the filtered Montmorillonite KSF, followed by extraction with CH_2Cl_2 to maximize the chemical yield. The subsequent straightforward methylation of the second OH group using iodomethane or dimethyl sulfate in DMF at 60 °C, following by the NaOH-mediated saponification led to the production of monomeric acidic building blocks **1k−1m**.

During the synthesis of **1q** from 2-hydroxy-5-methylbenzoic acid, bismuth nitrate-mediated nitration at room temperature tends to give inconsistent low chemical yields from time to time. It was finally realized that such nitration is highly sensitive toward both reaction temperature and reaction time. By controlling reaction temperature at −20 °C for 20 min, followed by immediate quenching with water, desired product can be obtained in a yield of as good as 80%. This bismuth nitrate-mediated nitration, surprisingly, did not work for **1r**. Its mononitration, however, can be accomplished using conc. HNO_3 and conc. H_2SO_4 in CH_2Cl_2, under which conditions, ironically, the nitration of **1b−1d** did not proceed at all. To facilitate the separation of mononitrated acid product **1r** from its isomer that contains a nitro group ortho to hydroxyl group and minor product containing two nitro groups, the reaction mixtures were converted to ester compounds. It is interesting to note that saturated $NaHCO_3$ can dissolve dinitro compounds, but not mononitro compounds, into the aqueous layer. The two mononitrated isomers thus can be efficiently separated by flash column chromatography using hexane/CH_2Cl_2 (v:v 4:1) as the eluent to give pure product **1r** as a bright-yellow solid.

Following the elaboration of the synthetic routes for the efficient preparation of various monomeric building blocks (Scheme 1: **1h−1m**, **1p**, **1s**, **1q** and **1t**), a series of oligoamides was prepared according to Schemes 2−4. A convergent route

(13) Qin, B.; Chen, X. Y.; Fang, X.; Shu, Y. Y.; Yip, Y. K.; Yan, Y.; Pan, S. Y.; Ong, W. Q.; Ren, C. L.; Su, H. B.; Zeng, H. Q. *Org. Lett.* **2008**, *10*, 5127.

(14) (a) Koert, U.; Harding, M. M.; Lehn, J.-M. *Nature* **1990**, *346*, 339. (b) Woods, C. R.; Benaglia, M.; Cozzi, F.; Siegel, J. S. *Angew. Chem., Int. Ed.* **1996**, *35*, 1830. (c) Orita, A.; Nakano, T.; An, D. L.; Tanikawa, K.; Wakamatsu, K.; Otera, J. *J. Am. Chem. Soc.* **2004**, *126*, 10389. (d) Katagiri, H.; Miyagawa, T.; Furusho, Y.; Yashima, E. *Angew. Chem., Int. Ed.* **2006**, *45*, 1741. (e) Zhang, F.; Bai, S.; Yap, G. P. A.; Tarwade, V.; Fox, J. M. *J. Am. Chem. Soc.* **2005**, *127*, 10590. (f) Dong, Z.; Karpowicz, R. J.; Bai, S.; Yap, G. P. A.; Fox, J. M. *J. Am. Chem. Soc.* **2006**, *128*, 14242. (g) Preston, A. J.; Gallucci, J. C.; Parquette, J. R. *Org. Lett.* **2006**, *8*, 5259.

Scheme 2. Synthesis of Trimers[a]

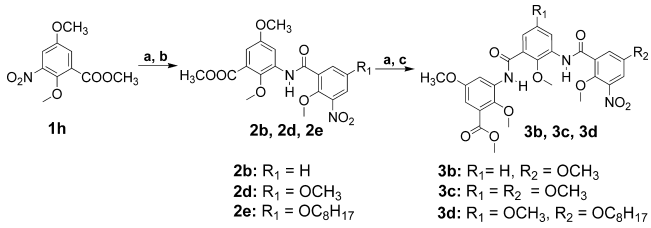

[a] Reagents and conditions: a) H_2, Pd/C, THF, 40 °C; b) ethyl chloroformate, 4-methylmorpholine, CH_2Cl_2, **1t** (for **2b**) or **1k** (for **2d**) or **1l** (for **2e**), RT; c) ethyl chloroformate, 4-methylmorpholine, CH_2Cl_2, **1k**, RT.

Scheme 3. Synthesis of Hexamer **6a**[a]

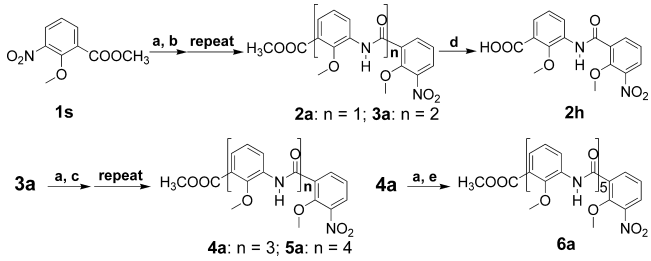

[a] Reagents and conditions: a) H_2, Pd/C, THF, 40 °C; b) ethyl chloroformate, 4-methylmorpholine, CH_2Cl_2, **1t**, RT, c) $(COCl)_2$, DMF, CH_2Cl_2, **1t**, then TEA/CH_2Cl_2; d) KOH, KCl, MeOH/H_2O, **2a,** reflux; e) ethyl chloroformate, 4-methylmorpholine, CH_2Cl_2, **2h**, RT.

was seldom used here because it either did not give the expected product or gave a low coupling yield (19% for **6a** by coupling tetramer **4a** with dimer **2h** and 6% for **6b** by coupling trimer **3a** with trimer **3g**). Instead, backbone construction (C-to-N) of the oligoamides **1**−**6** in a unidirectional stepwise fashion proved to be a more efficient, time-saving strategy by reacting monomeric active ester or acid chloride with amino-terminated oligoamides. This stepwise construction can be exemplified by the preparation of tetramer **4a** (Scheme 4). The synthesis of **4a** started from monomers **1s** and **1t**. Reduction of **1s** by Pd-/C-mediated hydrogenation at 40 °C in THF converted **1s** into amine intermediate that coupled with *in situ* generated active ester produced from **1t** (conditions: ethyl chloroformate, 4-methylmorpholine, CH_2Cl_2, room temperature) to give nitro-terminated dimer **2a** with a chemical yield of 71%. Hydrogenation of **2a** under the typical conditions (Pd/C, H_2, THF, 40 °C) produced amino-terminated intermediate that was subjected to the next coupling reaction with the above *in situ* generated active ester from **1t** to afford trimer **3a** with a chemical yield of 82%. Trimer **3a** was further hydrogenated (Pd/C, H_2, THF, 40 °C) to yield the corresponding amine intermediate that reacted with the acid chloride, which was generated from **1t** under the conditions involving oxalyl chloride and a few drops of DMF in CH_2Cl_2 at room temperature, to produce **4a** with a chemical yield of 61%.

Unfortunately, despite our numerous attempts, neither convergent nor stepwise synthesis was able to produce oligoamides of higher than hexamer, a reason why only the oligoamides of up to hexamers were presented and studied in the current work.

One-Dimensional ^{1}H NMR Studies of Oligoamides 2−6. The oligoamides **2**−**6** studied here contain three important sets of proton signals, i.e., amide protons, aromatic protons and interior methoxy protons. Among them, the chemical shift values of the amide protons are the simplest diagnostic of the existence of intramolecular H-bonds when compared to other more advanced analytical techniques (i.e., 2D NOESY and X-ray

Scheme 4. Synthesis of Oligomers from Dimers to Hexamers[a]

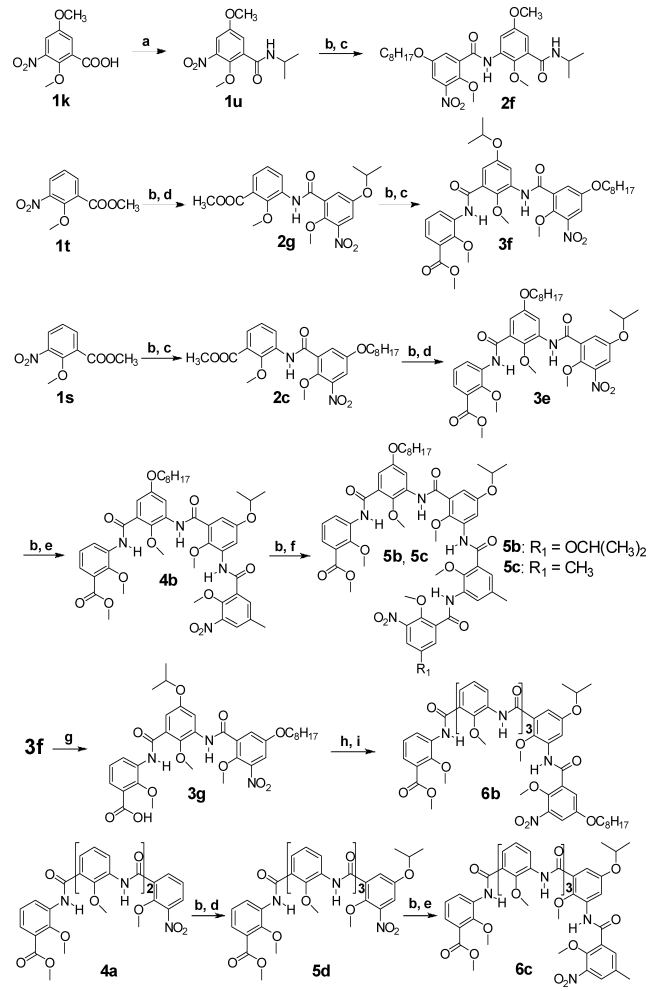

[a] Reagents and conditions: a) EDC, HOBT, propan-2-amine, CH_2Cl_2; b) H_2, Pd/C, THF, 40 °C; c) ethyl chloroformate, 4-methylmorpholine, CH_2Cl_2, **1l**; d) ethyl chloroformate, 4-methylmorpholine, CH_2Cl_2, **1m**; e) $(COCl)_2$, DMF, CH_2Cl_2, **1q**; f) $(COCl)_2$, DMF, CH_2Cl_2, **1m** (for **5b**) or **1q** (for **5c**); g) KOH, KCl, MeOH/H_2O, reflux; h) $(COCl)_2$, DMF, CH_2Cl_2; i) H_2, Pd/C, THF, 40 °C, **3a**, then TEA/CH_2Cl_2.

diffraction). In chloroform, upon forming intramolecular H-bonds, amide protons typically exhibit a substantial downfield shift due to the deshielding of amide protons by the adjacent electron-negative elements. The degree of downfield shifting thus provides a good indication as to the occurrence and strength of hydrogen bonds found in H-bond enforced aromatic foldamers. For example, amide protons involved in two-center H-bonds have a typical chemical shift of less than 9.6 ppm,[4f] while those involved in three-center H-bonds most often downfield shift much more than 10 ppm,[3d,4f,8,10a,b,e,13] suggesting that three-center H-bonds have a higher stability than two-center H-bonds of similar types.[10e]

The representative ^{1}H NMR spectra containing the amide and aromatic signals (Figure 1) for some selected oligomers are presented in Figure 1 with the chemical shifts for all the amide protons of the selected oligoamides **2**−**6** tabulated in Table 1. The majority of these amide protons resonant at >10 ppm at 1 mM in $CHCl_3$, a more than 1 ppm downfield shift than the amide proton (8.70 ppm) in **2f** and others[10b] that are involved in the formation of two-center H-bonds. This experimental observation is consistent with the expectation that these amide protons be engaged in a continuous intramolecular H-bonding network as

Table 1. Chemical Shifts (ppm)[a] and the Half-Lives (h, in parentheses) of H−D Exchange[b] of Amide Protons for Selected Oligomers **2**−**6**[c]

oligomer	H_6	H_{11}	H_{16}	H_{21}	H_{26}
2a	10.36 (0.13)				
2c	10.47 (0.90)				
3a	10.21 (0.04)	10.23 (0.27)			
3c	10.35 (0.08)	10.38 (1.34)			
4a	10.20 (0.63)	10.10 (0.03)	10.00 (0.06)		
4b	10.33 (0.92)	10.14 (0.11)	10.10 (0.08)		
5a	10.25 (0.33)	9.85 (0.05)	9.85 (0.20)	10.25 (0.27)	
5b	10.35 (1.90)	9.85 (0.07)	9.65 (0.28)	10.25 (0.37)	
6a	10.19 (0.07)	10.12 (0.09)	9.84 (0.06)	10.28 (0.11)	10.15 (0.38)
6b	10.12 (0.42)	10.08 (0.29)	9.81 (0.27)	10.21 (0.40)	10.09 (5.79)

[a] Chemical shifts were measured at 1 mM in $CDCl_3$ (500 MHz) at room temperature. [b] Half-lives of H−D exchange data in parentheses were measured at 5 mM in 5% D_2O/47.5% DMSO-d_6 (v:v) in $CDCl_3$ at room temperature. [c] For a complete list of chemical shifts and H−D exchange data of all the oligomers presented in this article, please see Supporting Information.

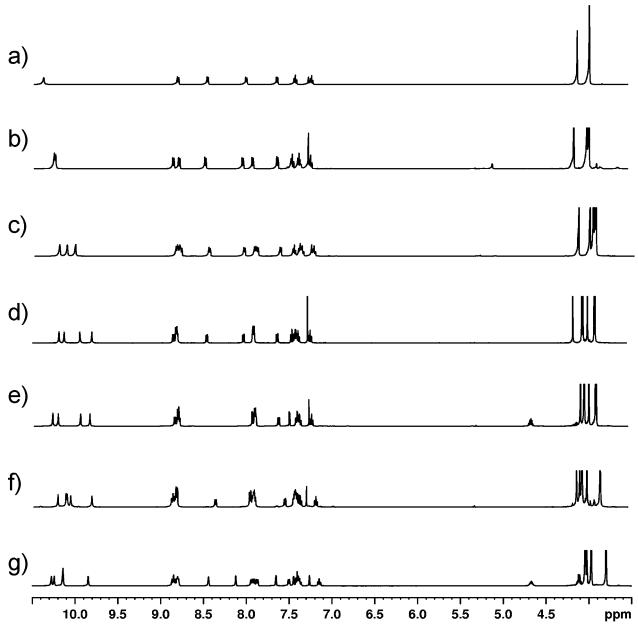

Figure 1. ^{1}H NMR (500 MHz) spectra of some selected oligomers **2**−**6** in $CDCl_3$ at 298 K: (a) dimer **2a** (20 mM), (b) trimer **3a** (10 mM), (c) tetramer **4a** (20 mM), (d) pentamer **5a** (5 mM), (e) pentamer **5c** (25 mM), (f) hexamer **6a** (20 mM), and (g) hexamer **6c** (20 mM).

originally conceived. The formed H-bonding network subsequently stabilizes the oligomers into a crescent-shaped well-defined conformation rather than a random coiled structure, giving rise to the sharp proton signals in all the spectra compiled in Figure 1.

Two-Dimensional ^{1}H NMR Studies (NOESY) of Oligoamides 2−6. Since NOE intensity is proportional to the inverse sixth power of the distance, the experimentally observed NOE intensity is largely determined by the shortest distance between two interacting nuclei. As revealed in the crystal structures of oligoamides **2**−**6**, the shortest interatomic distances between amide protons and the adjacent interior methoxy protons measure from 2.28 to 2.97 Å, an indication that the two NOE contacts between every amide proton and its adjacent methoxy methyl groups should be seen in the 2D NOESY spectrum if a folded conformation induced by intramolecular H-bonds does prevail for oligoamides **2**−**6** in solution.[15] Accordingly, the crescent-shaped or helically folded conformations in oligoamides **2**−**6** were probed by 2D NOESY studies (Figures 2 and 3). Due to the highly repetitive nature of oligoamides **2**−**6**, extensive ^{1}H NMR signal overlaps among aromatic protons were observed for an oligoamide as simple as trimer **3a**. This prevents the accurate and complete assignment involving the amide protons and adjacent interior methoxy methyl protons and so hampers the elucidation of their folded structures in solution. This issue was mostly solved by deliberately introducing linear and branched alkoxyl side chains as well as a methyl group para to the interior methoxy groups into oligoamides **2**−**6** (i.e., **2f**, **3d**, **4b**, **5b**, **5c**, **6b**, and **6c**). The introduction of these side chains indeed led to the well-resolved amide protons, aromatic protons, and internal methoxy groups in oligoamides **2f** (Figure 2a), **3d** (Figure 2b), and **5b**[8] that permit us to detect the expected two NOE cross-peaks for each amide protons. Additionally, the majority of these NOE intensities between interior methoxy protons and amide protons are much stronger than the weak NOE contacts between amide protons and the neighboring aromatic protons ortho to the amide bonds. For example, the NOE contact between protons *6* and *4* in pentamer **5c** is much stronger than that between protons *6* and *7* in the same molecule. This implies that the methoxy protons stay much closer to the amide protons than to the aromatic protons, which is a direct consequence resulting from the induced folding of the backbone by the internally located H-bonds. Compared to **4a** and **5a**, better ^{1}HNMR signal dispersions are also observed for **4b** (Figure 2c) and **5c** (Figure 2d), and some ^{1}H NMR peaks still either overlap substantially or display a small difference in chemical shift.

Previously, we have shown that oligomers of higher than tetramer such as **5a** and **6a** adopt a helical conformation in the solid state.[8] The inability to detect the NOEs between the end residues in pentamer **5c** in solution by 2D NOESY that are suggestive of its helical conformation is a fact that can be ascribed to its unusually large helical pitch (∼5 Å) as seen in the crystal structure of **5a**. Such a helical conformation, however, can be confirmed by 2D NOESY study for longer oligomers such as **6c** where the favorable $\pi-\pi$ stacking interactions between the first and sixth aromatic rings bring the two end residues closer to each other, leading to a typically observed helical pitch of ∼3.4 Å for aromatic foldamers.[3b−g] Correspondingly, a strong NOE cross-peak between the end ester methyl protons *1* and the aromatic proton *24* (Figure 3d−f), serving as

(15) For ortho-substituted isomers rigidified by only one H-bond (two such isomers can be generated for an oligomer as simple as **2a** by flipping one benzene ring to disrupt one H-bond while keeping the other intact), the distance between amide proton and protons of methoxy group whose oxygen atom is not involved in H-bond would be close to or larger than 5 Å. For methoxy group involved, one of its protons will be less than 3 Å away from the amide proton. This suggests that probably only one NOE can be detected for every amide proton for these two alternative isomers containing only one H-bond. Or conservatively, one strong and one very weak NOE should be seen. This differs from the isomers containing two H-bonds (i.e., three-center H-bonding system in **2a** or a continuous H-bonding network in oligomers **3**−**6**) where two NOEs with comparable intensities should be seen between every amide proton and its two neighboring methoxy methyl groups.

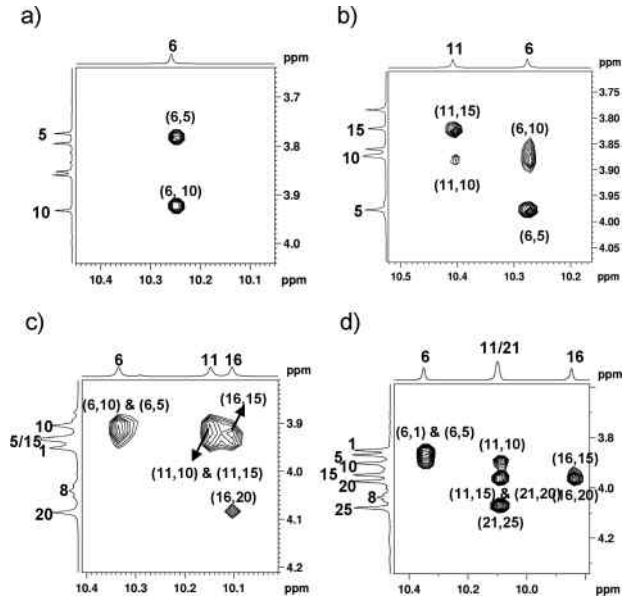

Figure 2. NOE contacts (NOESY, 500 MHz, 298 K, 10 mM, 500 ms, 4 h) seen between amide protons and their adjacent interior methoxy protons: (a) dimer **2f** in DMSO-d_6, (b) trimer **3d** in 50% $CDCl_3$/50% DMSO-d_6, (c) tetramer **4b** in $CDCl_3$, and (d) pentamer **5c** in $CDCl_3$.

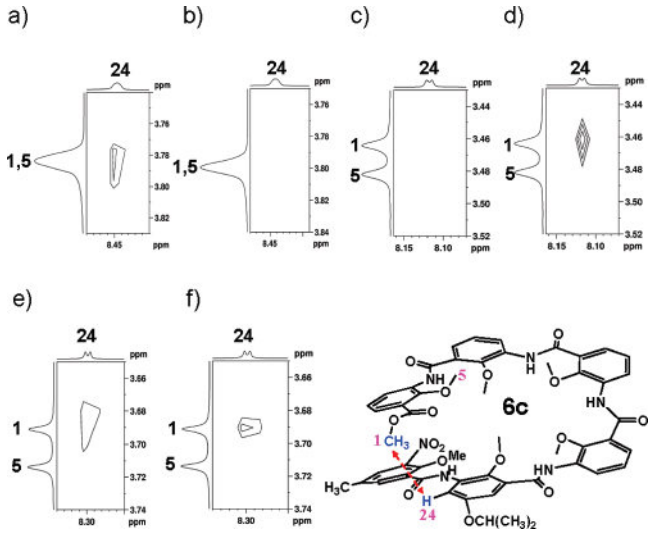

Figure 3. Two-dimensional (2D) NOESY (500 MHz, 10 mM, 500 ms) and ROESY (500 MHz 10 mM, 200 ms) studies of **6c**, showing end-to-end contact between protons *1* and *24* that is indicative of helical conformation. (a) 2D NOESY (283 K, $CDCl_3$, 4 h); (b) 2D NOESY (298 K, $CDCl_3$, 4 h); (c) 2D NOESY (283 K, $CDCl_3$/DMSO-d_6 (3:1 v/v), 4 h); (d) 2D NOESY (283 K, $CDCl_3$/DMSO-d_6 (3:1 v/v), 8 h); (e) 2D NOESY (298 K, $CDCl_3$/DMSO-d_6 (3:1 v/v), 8 h); and (f) 2D ROESY (298 K, $CDCl_3$/DMSO-d_6 (3:1 v/v), 4 h). Compared to that of (d), NOE peak intensity in (e) is much weaker.

an indicator for helical formation, was observed for **6c** at 10 mM in $CDCl_3$. The existence of this helical conformation can be nicely supported by the *ab initio* molecular modeling at the level of B3LYP/6-31G* (Figure 7c) and the determined crystal structure of **6a** (Figure 7b), both of which point to an energetically optimized configuration for **6c** where the six interior methoxy methyl groups point up and down alternatively along the aromatic backbone helically biased by a continuous H-bonding network.

It should be emphasized that before pentamer **5b** and hexamer **6b** were designed, synthesized, and reported by us recently,[8] pentamer **5c** and hexamer **6c** modified with various side chains were actually made first to probe the helical conformation that may be adopted by these longer oligomers. As seen from both its ^{1}H NMR spectrum (Figure 1f) and 2D NOESY study (Figure 2d), the side chains introduced into **5c** do not give rise to a complete resolution of amide protons and internal methoxy methyl groups. As to **6c**, although good end-to-end NOE contacts between either proton *1* or proton *5* and aromatic proton *24* can be detected in $CDCl_3$ at 283 K but not 298 K, the signal overlap between protons *1* and *5* makes the accurate assignment of ^{1}H NMR signals difficult. This issue can be solved by addition of up to 25% DMSO-d_6 into $CDCl_3$, leading to a good separation between protons *1* and *5* in both **6b** and **6c** (Figure 4). However, 2D NOESY collected for 4 h at 10 mM in 3:1 $CDCl_3$/DMSO-d_6 at either 283 or 298 K failed to yield detectable NOE contact between protons *1* and *24* in **6c**. Consequently, either crescent or helical conformation concerning oligomers **5c** and **6c** can not be confidently deduced. Before it was realized that lengthening the total acquisition time of 2D NOESY from 4 to about 8 h in 3:1 $CDCl_3$/DMSO-d_6 allows us to detect an end-to-end contact between proton *1* and proton *24* in **6c** (parts d and e of Figure 3), we decided to replace the methyl side chain at the nitro end with an isopropyloxy side chain to generate **5b** and with an octyloxy side chain to generate **6b**. Such a minute difference in structure pleasingly leads to completely resolved ^{1}H NMR signals for critically important protons that allow us to unambiguously confirm a crescent conformation for **5b** in pure $CDCl_3$ and a helical structure for **6b** in 3:1 $CDCl_3$/DMSO-d_6 at room temperature.[8] **6c** was also confirmed to assume a helical conformation in solution by a 2D NOESY experiment with a longer acquisition time (parts d and e of Figure 3) or by 2D ROESY study (Figure 3f).

Solid-State Structures of Oligoamides 2−4. Crystals of oligomers **2**−**4** suitable for X-ray structure determination were obtained by slow evaporation of these oligomers in mixed solvents at room temperature (Table 2). The top and side views of the determined crystal structures for oligoamides **2**−**4** are presented in Figure 5. These crystal structures demonstrate that with the stepwise addition of aromatic building blocks the elongated backbone becomes increasingly curved in one direction. This is a result of the stabilizing forces from the lengthened intramolecular H-bonding network that comprises up to six intramolecular H-bonds (NH···OMe = 1.933−2.306 Å). As reported recently by us,[8] a longer oligomer such as **5a** or **6a** with a long enough backbone eventually curves into a helical conformation as a result of the stabilizing H-bonding interactions, which more than compensate the unfavorable steric crowdedness involving the two interior methoxy end-groups.

A closer look into the crystal structures of oligoamides **2** and **3** reveals a quite surprising structural feature: while the aromatic rings in all four dimer molecules **2a**−**2d** are always coplanar, the nature of exterior side chains has an influential distorting effect on the planarity of the trimeric backbone in trimers **3a**−**3d** (Figure 6). This type of distortional behavior involving aromatic backbones is quite unusual and not seen in other H-bonded short aromatic oligomers of similar types.[3d,5m,10a,l,12a,16] As illustrated in Figure 6, the distortion angles (i.e., the dihedral angle formed between the plane defined by the first two benzene rings at the nitro end and the plane defined by the first benzene ring at the ester end) are 55° in **3a**, 30° in **3b**, 26° in **3c**, and 10° in **3d**. Interestingly, while the first two benzene rings at the nitro end

(16) Wu, Z.-Q.; Jiang, X.-K.; Zhu, S.-Z.; Li, Z.-T. *Org. Lett.* **2004**, *6*, 229.

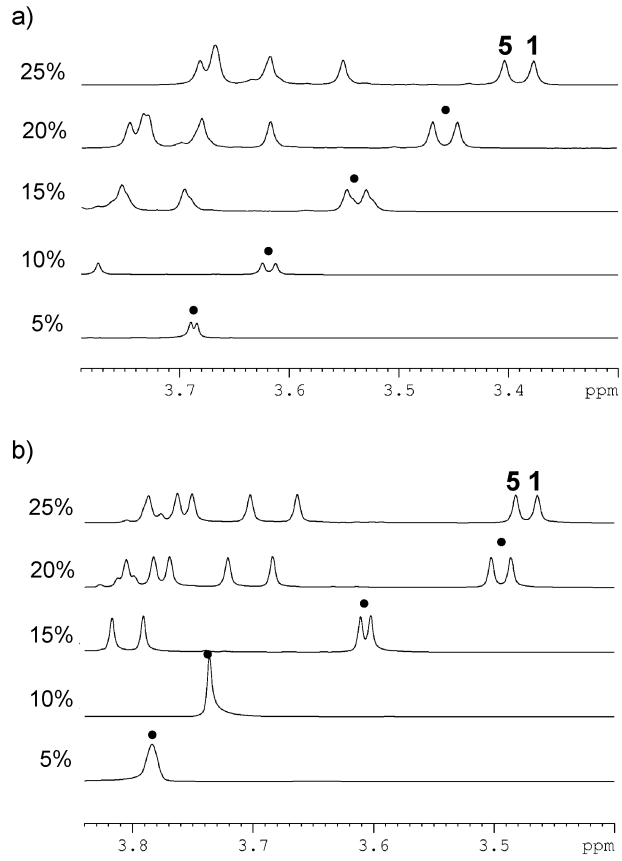

Figure 4. Effect of DMSO-d_6 percentage in $CDCl_3$ on the ^1H NMR signal dispersion involving protons *1* and *5* in (a) hexamer **6b** and (b) hexamer **6c**.

Table 2. Crystal Growth Conditions for Oligomers **2**−**4**

	solvent pair (1:1)		solvent pair (1:1)		solvent pair (1:1)
2a	CH_2Cl_2:MeOH	**2d**	$CHCl_3$:MeOH	**3c**	$CHCl_3$:hexane
2b	CH_2Cl_2:hexane	**3a**	$CHCl_3$:MeOH	**3d**	DMF:CH_3CN
2c	$CHCl_3$:MeOH	**3b**	CH_2Cl_2:hexane	**4a**	CH_2Cl_2:MeOH

stay coplanar in all the four trimer molecules **3a**−**3d**, all the distortions are fully concentrated around the amide linkage at the ester end whose *NH* proton *6* seems to form a much weaker six-membered H-bond than amide proton *11* at the nitro end. This weakness in H-bond strength can be inferred from amide hydrogen−deuterium exchange studies on protons *6* and *11* of trimers **3a**−**3f** (see Table 1, Figure 11, and the corresponding text) and can be further substantiated by theoretical calculations on the strength of the intramolecular H-bond in **3a** at the level of B3LYP/6-31G* (see Figure 12 and corresponding text). A

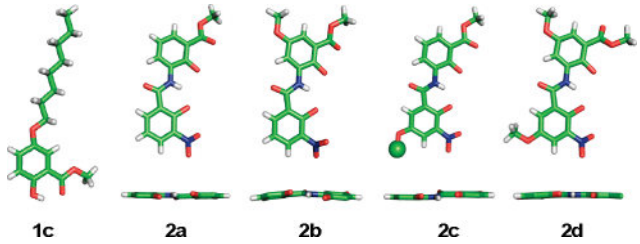

Figure 5. Crystal structure of intermediate **1c** as well as top and side views of crystal structure of **2a**−**2d**. In **2c**, the dummy atom represents the octyl side chain. In top views, all the interior methoxy methyl groups were removed for clarity of view. In side views, all the nitro groups, ester groups and side chains were removed for clarity of view.

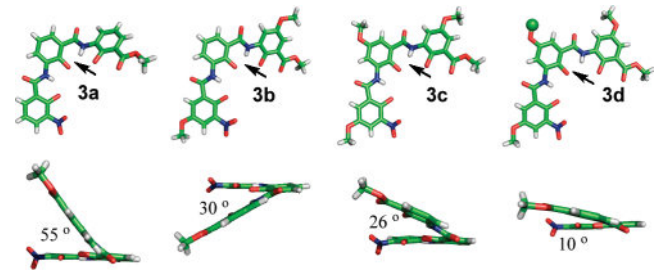

Figure 6. Top and side views of the crystal structures of **3a**−**3d**. The side views were generated by placing the nitro end in the back. In **3d**, the dummy atom represents the octyl side chain. All the interior methoxy methyl groups were removed for clarity of view. Solid arrows highlight the twisted six-membered H-bonds.

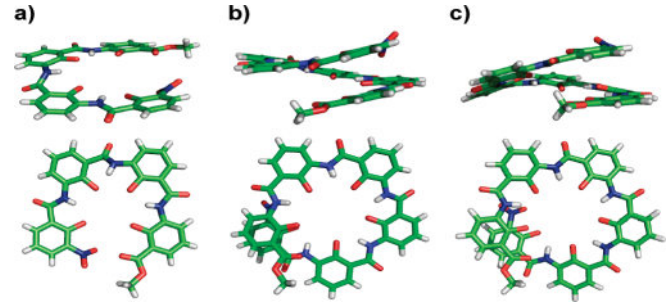

Figure 7. Top and side views of crystal structure of (a) **4a** and (b) **6a**.[8] The calculated structure of **6a** is shown in (c). All the interior methoxy methyl groups were removed for clarity of view.

need to maximize the favorable aromatic $\pi-\pi$ stacking interactions during the crystal packing likely is another decisive factor that contributes to such a deviation from the planarity (Figure 9). In other words, the intermolecular $\pi-\pi$ stacking interactions may override to a good extent the planarizing forces coming from the weaker H-bonds at the ester end, thereby causing the plane involving the weaker H-bonds to deviate significantly from the plane involving stronger H-bonds at the nitro end. A combination of $\pi-\pi$ interactions, the presence of amide proton *11* forming weak intramolecular H-bonds, repulsive interactions between end nitro and ester groups and steric hindrance among interior methyl groups shall account for the nonplanar aromatic backbone observed in tetramer **4a** (Figure 7a). Contrasting with both trimer and tetramer and as evidenced from their crystal structures, all the dimers **2a**−**2d** contain a strong three-center H-bond that forces the dimeric backbone defined by two aromatic rings and one amide bond into a perfectly coplanar geometry.

Examining the solid-state structures of dimers **2** (Figure 8) and trimers **3** (Figure 9) reveals a one-dimensional (1D) columnar assembly consisting of molecules packed in an antiparallel fashion via aromatic $\pi-\pi$ stacking interactions (interplane distances along the packing axis = 3.3−3.6 Å).[10l]

For dimers (except for **2b** that packs along diagonal axis $a-c$ forming an angle of 63° between axis $a-c$ and plane of the molecules) all of the other three dimers (**2a**, **2c**, and **2d**) are stacked along axis a with angles of 90°, 53°, and 70°, respectively, between axis a and plane of the molecules by virtue of aromatic $\pi-\pi$ interactions (Figure 8). These columns further assemble into 2D sheets and 3D structures via van der Waals interactions among aromatic C−H bonds, nitro groups, ester groups, and methoxy groups.

Three packing patterns can be observed for trimers. As shown in a−c of Figure 9, the stacking of **3a**−**3c** along axis a is mediated by aromatic $\pi-\pi$ interactions involving the first two

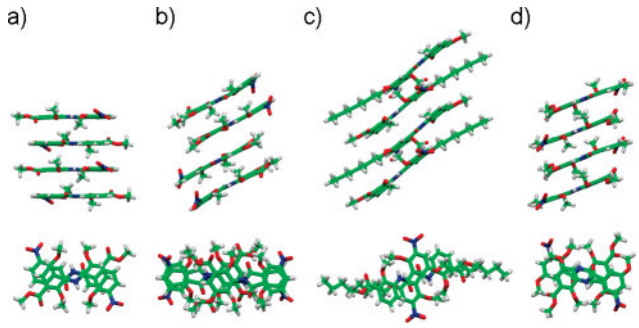

Figure 8. Side and top views of columnar assemblies observed in the solid-state structures of (a) **2a** along axis *a*, (b) **2b** along axis *a*−*c*, (c) **2c** along axis *a*, and (d) **2d** along axis *d*.

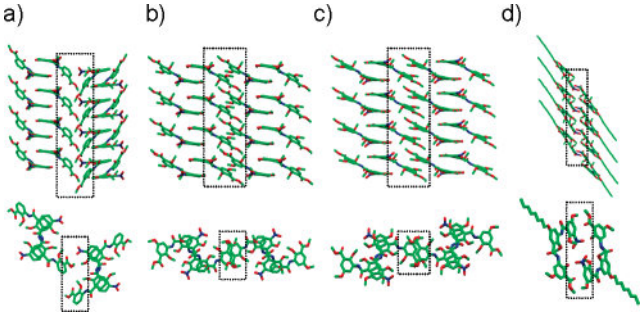

Figure 9. Side and top views of column formation and further association observed in the solid-state structures of (a) **3a**, (b) **3b**, (c) **3c**, and (d) **3d**. Dotted rectangles highlight the intercolumnar associations mediated by van der Waals and/or $\pi-\pi$ interactions. Hydrogen atoms are not shown.

benzene rings at the nitro end remaining coplanar. In **3d** (Figure 9d), the $\pi-\pi$ interactions between the central benzene ring and the end benzene ring close to the nitro group are responsible for associating the molecules into 1D columns along axis *a*. While the assembly of 1D columns into 2D/3D structures in both **3a** and **3d** (see dotted rectangles in a and d of Figure 9) does not involve $\pi-\pi$ stacking, $\pi-\pi$ interactions do play an important role in driving the intercolumnar assemblies in the solid-state assembly of both **3b** and **3c** (see dotted rectangles in b and c of Figure 9). Additionally, among the eight oligomers **2a**−**2d** and **3a**−**3d**, only **3d** packs in a parallel fashion along the stacking axis.

The consistent columnar assembly of the above short oligomers **2**−**3** in solid states suggests that, with their cavity-containing backbones, oligomers longer than trimer may be capable of stacking on top of one another into channel-like structures. This possibility was first examined by the solid-state structure of **4a**. As expected, the molecules of **4a** stack into a channel that is stabilized by $\pi-\pi$ interactions along the *c* axis of the unit cell (see dotted red oval shape in Figure 10a). Re-examining the crystal structures of **5a** and **6a** reveals similar channels in the solid state (see dotted red circle or oval shape in parts b and c of Figure 10). The side views of these channels along axis *b* for **4a**, approximately along axis *b* for **5a**, and along axis *c* for **6a** show that all the channels are stabilized by $\pi-\pi$ interactions through partial overlap of aromatic backbones. Although the interiors of the channels formed by **4a**−**6a** are decorated by oxygen atoms, the presence of hydrophobic methoxy methyl groups must obstruct the channels' ability to conduct inorganic species such as Na^+ and K^+. Nevertheless, given the fact that **4a**−**6a** all enclose a small cavity radius of ∼2.8 Å from the center of the cavity to the nucleus of the interior oxygen atom and that coordination distances between

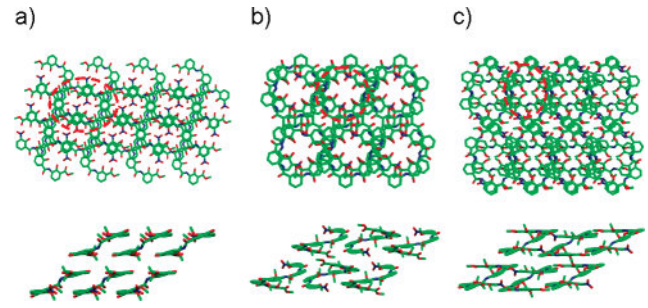

Figure 10. (Top) Channel formation observed in the solid state structures of (a) **4a**, (b) **5a**, and (c) **6a**. (Bottom) Side views illustrating $\pi-\pi$ interactions that lead to the channel formation in **4a**−**6a**. Dotted oval shapes or circles in red highlight one repeating channel unit. For clarity of view, some methoxy methyl groups inside the channels were removed.

the oxygen atom and the majority of metal cations fall below 2.8 Å, we hypothesize that replacing the interior methoxy groups with phenolic hydroxyl groups and subsequent deprotonation of hydroxyl group will restore the oxygen's ability to bind metal ions. The resultant channels will be able to bind/stabilize partially or fully dehydrated metal ions and subsequently allow the flow of ions under applied electrochemical gradients (i.e., concentration or voltage gradient).[10m] This theory is being pursued and will be reported in due course.

Amide Hydrogen−Deuterium (H−D) Exchange Studies on the Oligoamides 2−6. The H−D exchange of amide protons can be detected by ^{1}H NMR and has been used as a general method to distinguish between intramolecularly H-bonded and solvent-exposed amide moieties in biological settings such as α-helices and β-sheets. In H−D exchange experiments, the solvent-exposed amide protons are continually exchanging with the solvent molecules such as D_2O and usually are replaced much faster by deuterium atoms than their H-bonded counterparts, leading to the considerably shorter H−D exchange half-life. Similarly, protons that are involved in weaker H-bonds are exchanged faster with a shorter half-life than those forming stronger H-bonds if these protons are accessible equally well by solvent molecules. Consequently, amide H−D exchange experiments offer a sensitive reflection of the H-bond strength of amide protons as well as their solvent exposure degree. Very recently, this method was applied to both H-bond detection and quantitative measurement of H-bond strength in some aromatic foldamers by Gong[10e] and us.[13] A H−D experiment can be initiated by adding a 50 μL of D_2O into 0.95 mL of 5 mM oligomer in deuterated solvents containing $CDCl_3$:DMSO-d_6 (v:v 1:1), followed by monitoring a change in the integration of amide proton signals at the appropriate time intervals and fitting the obtained time-dependent integration change into a pseudo-first-order rate equation to derive the half-life of the amide protons.

Under the presently used H−D exchange conditions, the half-lives of all the amide protons in oligoamides **2**−**6** have been determined at 5 mM and selectively compiled in Table 1. Given the overall dimensionality of **2**−**6**, sticking-out orientation of interior methyl groups, and a low concentration of 5 mM used for amide H−D exchange experiment, the intermolecular aggregation for all the studied oligoamides is a highly unlikely event in solution. Thus, for short oligoamides including dimers **2a**−**2g**, trimers **3a**−**3g**, and tetramers **4a**−**4b**, the relative values of H−D half-lives should reflect the relative stabilities of H-bonds; for longer oligomers such as pentamers and hexamers that take up a helical conformation, amide H−D exchange shall

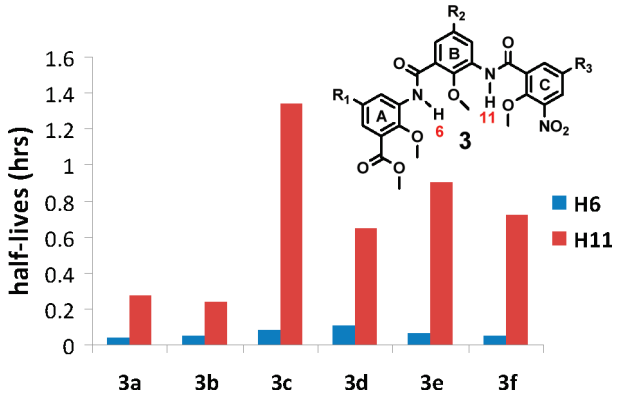

Figure 11. Half-lives of hydrogen−deuterium exchange rate for the amide protons *6* and *11* in trimer **3**. See Table 1 for the conditions and Supporting Information for the half-lives of all the other amide protons in oligomers **2**−**6**. Depending on R_1−R_3, plane *A* is twisted by varying degrees from the plane defined by planes *B* and *C* that remain coplanar.

be additionally affected by a steric factor arising from the end-to-end overlapping as observed in helical structures **5a** and **6a**.[8] In this regard, comparison of H−D exchange values among the short oligomers of the same length such as dimers **2a**−**2g**, trimers **3a**−**3g**, or tetramers **4a**−**4b** shows that the exteriorly located electron-donating side chains (1) cause a large variation in H-bond strength and (2) result in intramolecular H-bonds in oligomers modified with exterior side chains stronger than those found in the oligomers **2a**−**4a** that carry no side chains. Although an increase in H-bond strength involving proton *6* in **5b** and **5c** cannot be excluded, the observation of H−D exchange half-lives for proton *6* in **5b** ($t_{1/2}$ = 1.90 h) and **5c** ($t_{1/2}$ = 1.25 h) much larger than that in **5a** ($t_{1/2}$ = 0.33 h) may indicate that the presence of exterior side chains make proton *6* in **5b** and **5c** less accessible by D_2O molecules than the same proton in **5a**. Similarly, comparison of H−D exchange values for proton *26* in **6a** ($t_{1/2}$ = 0.38 h), **6b** ($t_{1/2}$ = 5.79 h), and **6c** ($t_{1/2}$ = 1.20 h) shall allow us to surmise that proton *26* in **6b** and **6c** that both contain two exterior side chains on the nitro end is much less solvent-exposed than proton *26* in **6a** that contains no exterior side chains.

Of particularly interest are the amide H−D exchange behaviors of the two amide protons found in trimers **3a**−**3g** (Figure 11): the half-lives of H−D exchange rate for the amide proton *6* in all the studied trimers fall within a narrow range of 0.04−0.11 h that is significantly much smaller than those for proton *11* (0.27−1.34 h) in the same molecules. This suggests to us that the amide group involving proton *6* shall constitute a conformationally weak point along the H-bonded aromatic backbone of these trimer molecules. This reasoning is in an excellent agreement with the backbone distortion fully centered around proton *6* as observed in the solid-state structures of **3a**−**3d** (Figure 6) and can be further supported by the theoretically determined relative H-bond strengths for all four intramolecular H-bonds found in trimer **3a** (Figure 12). A further examination on H−D exchange data (Figure 11) shows that the H-bonding strength involving proton *6* increases in the order of **3a**, **3b**, **3c**, and **3d**, which is surprisingly consistent with the observation that the distortional dihedral angle decreases in the order of **3a**, **3b**, **3c**, and **3d** (Figure 6).

Computational Studies on Oligoamides 3a and 6a. *Ab initio* molecular modeling with the B3LYP/6-31G* basis set has consistently allowed us to reliably predict the 3D topography of a circular pentamer[13] and an acyclic helical pentamer **5a**[8]

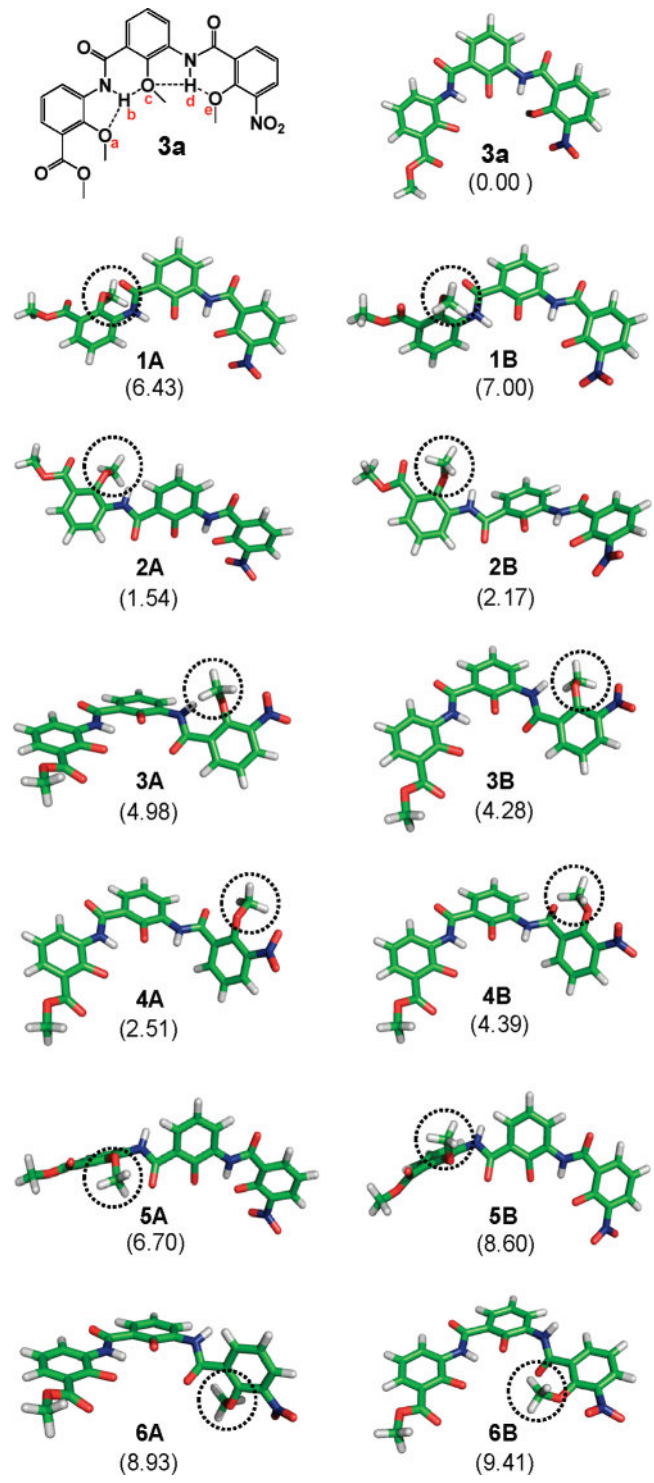

Figure 12. *Ab initio* (B3LYP/6-31G*) optimized conformers derived from **3a** and generated by breaking the H-bonds of $O_a\cdots H_b$ (**1A** and **1B**), $H_b\cdots O_c$ (**2A** and **2B**), $O_c\cdots H_d$ (**3A** and **3B**), and $H_d\cdots O_e$ (**4A** and **4B**), and by breaking H-bonds of both $O_a\cdots H_b$ and $H_b\cdots O_c$ (**5A** and **5B**), and both $O_c\cdots H_d$ and $H_d\cdots O_e$ (**6A** and **6B**), while keeping the rest of the H-bonds intact. For each category, two conformers were calculated that differ from each other only by the orientation of the cyclized methoxy methyl group. Shown in parentheses is the calculated relative energy (kcal/mol) normalized against the most stable conformer **3a**. For clarity of view, two interior methyl groups were omitted for each conformer.

and many others that are to be reported. As discussed above, amide proton *6* in trimers **3a**−**3d** is involved in the relatively weaker H-bonding interactions than those of proton *11* and

Table 3. Depending on the Spatial Orientations Involving Interior Methoxy Methyl Groups, a Total of 10 Conformations (**I**−**X**) Were Selected and Calculated for Acyclic Hexamer **6a** at the Level of B3LYP/6-31G*[a]

conformers	interior side chain orientation (starting from ester end in **6a**)	relative energy (kcal/mol)
I	up−down−up−down−up−down	0.00
II	up−down−down−down−up−down	2.46
III	down−down−up−down−up−down	2.71
IV	up−down−up−up−up−down	3.78
V	down−up−down−up−down−down	3.90
VI	up−up−up−down−up−down	4.19
VII	down−up−down−up−down−up	4.62
VIII	up−down−up−down−down−down	4.70
IX	down−down−up−down−down−down	5.10
X	down−down−down−down−down−down	9.09

[a] The modeling results on these conformers suggest that conformer **I** is the most stable conformation among the 10, and the only conformation that is seen in the crystal structure of **6a**.

becomes the "battle of the bulge" where the backbone readily gets twisted out of the planarity. To understand this focused twisting, we carried out the *ab initio* calculation at the level of B3LYP/6-31G* on a total of eight conformers (**1A**−**4A** and **1B**−**4B** in Figure 12) generated by alternatively flipping/rotating one benzene ring to disrupt one H-bond while keeping the remaining three H-bonds intact and by a further subtle adjustment on the interior methoxy side-chain orientation while keeping the rest of the molecule identical to the most stable conformer **3a** as much as possible. From the results gathered in Figure 12, it can be seen that the six-membered intramolecular H-bond involving proton *6* (or proton *b* in **3a** of Figure 12) is the weakest: breaking this H-bond possibly requires an energy input of 1.54−2.17 kcal/mol (conformers **2A** and **2B** in Figure 12), while the other three intramolecular H-bonds may need 2.51−7.00 kcal/mol with the five-membered intramolecular H-bond at the ester end being the most stable (6.25−7.00 kcal/mol, conformers **1A** and **1B**). It can also be seen that breaking the first two H-bonds (6.70−8.60 kcal/mol, conformers **5A** and **5B**) at the ester end is energetically easier than the first two H-bonds at the nitro end (8.93−9.41 kcal/mol, conformers **6A** and **6B**) that maintains the coplanarity involving the two aromatic rings at the nitro end as seen in the crystal structures of **3a**−**3d**. These calculations imply that the H-bond strength is highly likely to increase in the order of $H_b\cdots O_c < H_d\cdots O_e < O_c\cdots H_d < O_a\cdots H_b$.

To probe the possible solution conformations adopted by higher oligomers such as hexamers **6a**−**6c** and also to elucidate the effect of the interior methoxy side-chain orientation on the energetic profiles of their various conformers, a detailed calculation on hexamer **6a** was also performed. Thus, a total of 10 conformations (**I**−**X**) were generated and fully optimized that are dependent on the relative orientations of the six interior methoxy methyl groups. The modeling results on these 10 conformers are tabulated in Table 3. An energy minimum is found for hexameric conformer **I** bearing six methoxy groups spatially arranged in an up−down−up−down−up−down fashion; its computationally calculated structure is presented in Figure 7c. All the other nine conformers **II**−**X** with other alternative side-chain orientations are energetically less stable by 2.46−9.09 kcal/mol. The minimum-energy conformer **I** adopts a helical geometry with an appreciable interior cavity of slightly larger than 1.4 Å that is filled by the methoxy methyl groups. As compared in Figure 7, the calculated 3D topography and cavity of **6a** (Figure 7c) closely resemble those features observed in its solid-state structure (Figure 7b).

Conclusion

To summarize, the utilization of internally located H-bonds to rigidify the amide linkages and thus the aromatic backbone is a viable strategy that has allowed a series of single-stranded molecular strands to fold into crescent or helical conformations in both solution and solid state. Such a molecular folding process driven primarily by H-bonding is independent of the exterior side chains and proceeds in both nonpolar and polar solvents such as DMSO. A combination of *ab initio* molecular modeling with the amide H−D exchange data provides a good explanation and important hints at the origin of the localized backbone distortion as seen in the solid-state structures of four trimer molecules that shall result from the weakened hydrogen-bonding strength in combination with the $\pi-\pi$ stacking interactions. Our current investigations have also demonstrated the consistent columnar packing of these shape-persistent crescent oligoamides containing convergently arranged oxygen atoms that are essential for cation binding. These results have provided the basis for the follow-up study and elucidation of the higher ordered structures of these folding molecules with interesting properties and applications.

Many aspects of the synthetic chemistry associated with this class of backbone-rigidified oligomers are also established that should greatly facilitate designing and synthesizing other interesting oligomers functionalized with various tailor-made side chains for the uses as advanced functional materials. By taking advantage of a protecting group-driven synthesis reported by Gong,[10i] oligomers higher than hexamer may be produced. By selectively substituting some interior methoxy groups in such as **4a**, **5a**, and **6a** with hydroxyl groups and deprotonating the resulting phenolic hydroxyl groups, the helical cavity in **4a**−**6a** may open up for helically wrapping cations of varying types (i.e., Na^+ and K^+) and subsequent passage of metal ions through the channels. Effort along this line is being pursued.

Acknowledgment. This work was financially supported by the AcRF Tier 1 Grants (R-143-000-375-112 and R-143-000-398-112).

Supporting Information Available: A complete list of the chemical shifts and H−D exchange half-lives for the amide protons in oligomers **2**−**6**, synthetic procedures along with a full set of characterization data including P^1PH, $P^{13}PC$, and HRMS as well as CIF files (dimers **2a**−**2d**, trimers **3a**−**3d**, tetramer **4a**, pentamer **5a**, and hexamer **6a**), and details on amide H−D exchange and molecular modeling. This material is available free of charge via the Internet at http://pubs.acs.org.

JA100579Z